

# Phonon modes of $\text{ZnS}_{1-x}\text{Te}_x$ alloys epitaxially grown on (100) GaAs substrates

C. X. Jin, Z. Ling, D. H. Wang, D. M. Huang, X. Y. Hou, and Xun Wang<sup>a)</sup>  
*Surface Physics Laboratory, Fudan University, Shanghai 200433, People's Republic of China*

(Received 3 October 1996; accepted for publication 2 January 1997)

$\text{ZnS}_{1-x}\text{Te}_x$  ( $0 < x < 1$ ) alloys grown on (100) GaAs substrates by molecular beam epitaxy are investigated using the x-ray diffraction and Raman scattering. The frequencies of long wavelength ZnTe-like and ZnS-like longitudinal optical phonons determined from Raman scattering show linear variation with the composition  $x$ . The frequency of the zone-center optical phonons as a function of  $x$  of the  $\text{ZnS}_{1-x}\text{Te}_x$  mixed crystal shows a typical two-mode behavior, which is in good agreement with the theoretical results from a modified random-element isodisplacement model. © 1997 American Institute of Physics. [S0021-8979(97)03707-9]

## I. INTRODUCTION

Wide band-gap II–VI semiconductors, especially ZnSe and its related ternary and quaternary alloys such as ZnCdSe, ZnSSe, and ZnMgSSe, are currently the major constituent materials of the ZnSe-based blue-green laser diodes, and thus have been extensively investigated in the last few years. On the other hand, little attention has been paid to  $\text{ZnS}_{1-x}\text{Te}_x$  alloy, although its band-gap energy spans the entire visible and near-ultraviolet (UV) range (2.26–3.60 eV), making it a promising material for short wavelength optoelectronic devices.

Earlier studies of  $\text{ZnS}_{1-x}\text{Te}_x$  alloys were performed on thin films deposited on a Si substrate using electron beam evaporation,<sup>1</sup> and rf sputtering.<sup>2,3</sup> The electron beam evaporated films were polycrystals, while the rf sputtered films were grown in the islanding growth mode, resulting in unsatisfactory crystalline qualities for the purpose of basic physics studies and device applications. Wong and co-workers have successfully grown  $\text{ZnS}_{1-x}\text{Te}_x$  epitaxial films using molecular beam epitaxy (MBE),<sup>4,5-6</sup> and have observed strong photoluminescence in the yellow to blue region of the spectrum with external quantum efficiencies of 2%–4% at room temperature. High resolution x-ray diffraction, optical transmission, and photoluminescence (PL) spectra have been employed to characterize structural quality, chemical composition, the band-gap, and the Stokes shift of the PL peak.

In this work, the vibrational properties of  $\text{ZnS}_{1-x}\text{Te}_x$  alloys are studied using Raman spectroscopy. The Raman frequencies measured for different compositions provide information of the two-mode behavior of the phonon system. The frequencies of the zone-center optical phonons as a function of  $x$  are calculated using a modified random-element isodisplacement (MREI) model. The results are in good agreement with the experimental data. It is suggested that the measurement of the ZnS-like phonon frequency provides a simple and accurate way to characterize the composition of ternary alloys.

## II. EXPERIMENT

All samples used in this study were grown by MBE on (100) GaAs substrates. The substrate was treated with conventional chemical etching in  $5\text{H}_2\text{SO}_4:1\text{H}_2\text{O}_2:1\text{H}_2\text{O}$  solution, followed by rinsing in de-ionized water. After being loaded into the growth chamber, the substrates were heated to 580 °C for 5 min to remove the native oxides on the surface, and cooled to 280 °C for MBE growth. Elemental source materials of Zn (6N), Te (6N) and compound ZnS (6N) were used for the MBE growth. The source temperatures of Zn and Te were kept at 250 and 270 °C, respectively, during growth, whereas the temperature for ZnS was varied from 800 to 850 °C to obtain different compositions of the  $\text{ZnS}_{1-x}\text{Te}_x$  epilayers. The background pressure on the growth chamber was below  $2 \times 10^{-9}$  Torr and the pressure during the growth remained below  $2 \times 10^{-8}$  Torr. The nominal thicknesses of epilayers were 1000–2000 nm.

X-ray diffraction was performed on a D/MAX-YB x-ray diffractometer with Cu  $K\alpha$  radiation as the source to determine the structures and the lattice constants of the epilayers. The Raman spectra were obtained at room temperature in near backscattering geometry. The 488.0 nm line of an  $\text{Ar}^+$  laser was used as the source of excitation. The scattered light was dispersed by a Jobin-Yvon U1000 double monochromator and detected by a cooled photomultiplier. The polarization of the incident beam was fixed. The scattered beam was analyzed by a Polaroid sheet combined with a half-wave plate placed in front of the entrance slit, so that the spectra with two different polarization geometries,  $x(y,z)x$  and  $x(y,y)x$ , can be recorded, where  $x$ ,  $y$ , and  $z$  denote the coordinates of the (100), (010), and (001) directions with respect to the (100) GaAs substrate. The spectral slit width was  $2.0 \text{ cm}^{-1}$ .

## III. RESULTS AND DISCUSSION

Figure 1 shows the x-ray diffraction spectra of several samples with different alloy compositions. The peaks labeled  $S_1$ ,  $S_2$ , and  $S_3$  correspond, respectively, to the (200), (400), and (600) reflections from the GaAs substrate. The peaks labeled  $Z_1$ ,  $Z_2$ , and  $Z_3$  are the (200), (400), (600) diffraction peaks, respectively, from  $\text{ZnS}_{1-x}\text{Te}_x$  epilayers. The x-ray

<sup>a)</sup>Electronic mail: xunwang@fudan.ihep.ac.cn

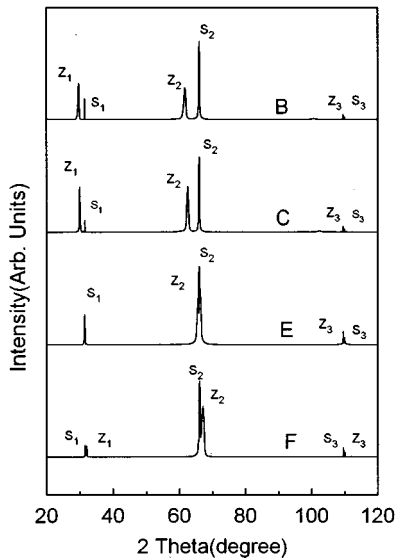


FIG. 1. The x-ray diffraction spectra of  $\text{ZnS}_{1-x}\text{Te}_x$  epilayers with different compositions. Peaks  $S_1$ ,  $S_2$ , and  $S_3$  are from the GaAs substrate, while the peaks  $Z_1$ ,  $Z_2$ , and  $Z_3$  are from  $\text{ZnS}_{1-x}\text{Te}_x$  epilayers.

diffraction spectra clearly show that the  $\text{ZnS}_{1-x}\text{Te}_x$  epilayers are single crystal with zinc-blende structures in the entire composition range of  $0 < x < 1$ .

The lattice constant can be determined from the shifts of the diffraction peaks with respect to those of the GaAs substrate. In an alloy with zinc-blende structure, the composition is directly related to the lattice constant according to Vegard's law, which is given by  $a(x) = 5.410 + 0.693x$  for  $\text{ZnS}_{1-x}\text{Te}_x$ .<sup>4</sup> The lattice constants and the compositions of our samples derived from x-ray diffraction and Vegard's law are listed in Table I. Also listed are the thicknesses of the epilayers and the critical thicknesses of pseudomorphic growth calculated from the mechanical equilibrium theory proposed by Matthews.<sup>7</sup> It can be seen that only the thickness of sample E is smaller than its critical thickness. Thus sample E is fully strained. Since its lattice mismatch to the substrate is quite small, the strain effect on the frequency shift of the optical vibration is estimated to be about  $0.8 \text{ cm}^{-1}$  and thus could be neglected in the following analysis of its Raman data. The other samples are expected to be fully relaxed, thus no strain effect should be taken into account. In Fig. 1, no diffraction peak from other phases is observed and

TABLE I. The lattice constant ( $a$ ), composition ( $x$ ), lattice misfit to GaAs ( $f$ ), thickness ( $d$ ), and corresponding critical thickness ( $d_c$ ) of  $\text{ZnS}_{1-x}\text{Te}_x$  samples.

Sample	$a$ (Å)	$x$	$f$ (%)	$d$ (nm)	$d_c$ (nm)
A	6.102	1.00	7.92	1500	4.0
B	6.004	0.86	6.21	1000	5.5
C	5.930	0.75	4.92	1000	7.0
D	5.840	0.62	3.28	2000	15
E	5.638	0.33	0.26	1000	1500
F	5.576	0.24	1.37	2000	40
G	5.410	0.00	4.31	80	10

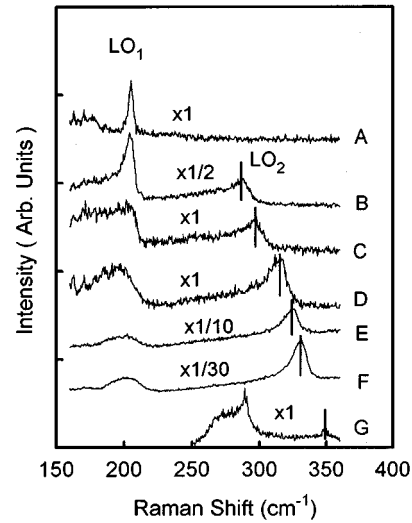


FIG. 2. Raman spectra of the  $\text{ZnS}_{1-x}\text{Te}_x$  samples.

the peak width [full width at half-maximum (FWHM)] of the epilayers is comparable to that of the substrates.

Figure 2 shows the Raman spectra of samples A–G. The peaks labeled [longitudinal optical (LO)]  $\text{LO}_1$  at around  $200 \text{ cm}^{-1}$  are identified as the ZnTe-like LO phonons, and the peaks labeled  $\text{LO}_2$  between  $278$  and  $350 \text{ cm}^{-1}$  are from the ZnS-like LO phonons. Peak  $\text{LO}_1$  shifts slightly towards higher frequencies as the Te content increases, whereas the frequency of peak  $\text{LO}_2$  phonons shows a remarkable redshift as the Te content increases. For samples A and G ( $x=1$  and  $0$ ), the frequencies of the LO phonons are found to be  $205 \text{ cm}^{-1}$  (ZnTe, LO) and  $348 \text{ cm}^{-1}$  (ZnS, LO), respectively. The ZnTe-like LO ( $\text{LO}_1$ ) phonon mode dominates the Raman spectra of samples with larger Te compositions, while samples with lower Te compositions show the dominant feature of the ZnS-like LO ( $\text{LO}_2$ ) phonon mode. A weak peak labeled  $\text{TO}_1$  is assigned to the zone-center ZnTe-like ( $\text{TO}_1$ ) transverse optical (TO) phonon, since it is not observed in the ZnS film (sample G). The selection rules for nearly back-scattering configuration from the (100) surface in a zinc-blende structure allow only the signals originated from LO but not those from TO phonons. The appearance of the TO phonon in the spectra is attributed to the relaxation of the  $q$  conservation law in the scattering process that is due to alloy disorder or light misorientation of the samples.<sup>8</sup> In sample G, the peaks at  $290$  and  $269 \text{ cm}^{-1}$ , which are absent in other samples, are believed to be originated from the LO and  $\text{LO}^-$  phonons of the GaAs substrate. The larger intensity of the LO phonon peak from the GaAs substrate than that from the ZnS epilayer is mostly the result of the very small thickness of the ZnS epilayer ( $80 \text{ nm}$ ). The frequencies of long-wavelength ZnTe-like and ZnS-like optical phonons measured from Raman spectra are plotted as dots in Fig. 3.

Similar studies were previously performed on some ternary III–V semiconductor alloys, such as  $\text{Ga}_{1-x}\text{Al}_x\text{As}$ ,<sup>9</sup>  $\text{Al}_{1-x}\text{In}_x\text{As}$ ,<sup>10</sup> and  $\text{Ga}_{1-x}\text{In}_x\text{As}$ ,<sup>11</sup> and some II–VI semiconductor alloys, such as  $\text{Zn}_{1-x}\text{Cd}_x\text{S}$ ,<sup>12</sup>  $\text{ZnS}_x\text{Se}_{1-x}$ ,<sup>13</sup>  $\text{Zn}_{1-x}\text{Mg}_x\text{Se}$ ,<sup>14</sup> and  $\text{Zn}_{1-x}\text{Mn}_x\text{Te}$ .<sup>15</sup> It was also demonstrated that the optical phonon frequency as a function of  $x$  in

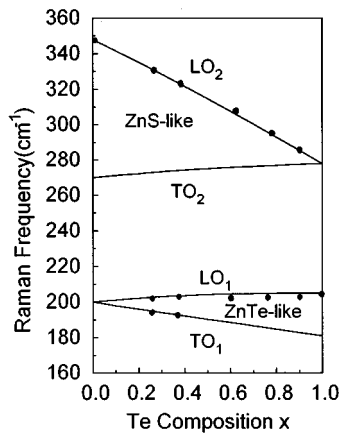


FIG. 3. The frequencies of long-wavelength optical phonons in  $\text{ZnS}_{1-x}\text{Te}_x$  as a function of  $x$ . The dots are the experimental data and the solid lines are calculated with the MREI model.

a mixed crystal  $AB_{1-x}C_x$  exhibits either one-mode type (such as  $\text{Zn}_{1-x}\text{Cd}_x\text{S}$ ),<sup>12</sup> two-mode type [such as  $\text{Ga}_{1-x}\text{Al}_x\text{As}$ ,<sup>9</sup>  $\text{Al}_{1-x}\text{In}_x\text{As}$ ,<sup>10</sup>  $\text{Ga}_{1-x}\text{In}_x\text{As}$ ,<sup>11</sup>  $\text{ZnS}_x\text{Se}_{1-x}$ ,<sup>13</sup> and  $\text{Zn}_{1-x}\text{Mg}_x\text{Se}$  (Ref. 14)] or intermediate-mode type [such as  $\text{Zn}_{1-x}\text{Mn}_x\text{Te}$  (Ref. 15)] behavior depending on the masses of A, B, and C atoms. According to the MREI model proposed by Chang and Mitra<sup>16</sup> and Peterson *et al.*,<sup>15</sup> a two-mode mixed crystal must have one substituting element whose mass,  $m_B$  ( $m_C$ ), is smaller (larger) than the reduced mass of the compound formed by the other two elements,  $\mu_{AC}$  ( $\mu_{AB}$ ).<sup>16</sup> For  $\text{ZnS}_{1-x}\text{Te}_x$ , the mass of S (32.06) is smaller than the reduced mass of ZnTe (43.23), and the mass of Te (127.63) is larger than the reduced mass of ZnS (21.51). It is thus expected that  $\text{ZnS}_{1-x}\text{Te}_x$  should possess two-mode behavior. A calculation of the composition dependence of the Raman frequency was carried out using the MREI model. The fundamental assumptions of the MREI model are that in the long-wavelength limit ( $q \sim 0$ ), the anions and the cations of like species vibrate with the same phase and amplitude and that the force experienced by each ion is provided by a statistical average of the interaction with its neighbors. The parameters used in the calculations are as follows. For ZnTe,  $\omega_{\text{TO}}(\text{ZnTe}) = 181 \text{ cm}^{-1}$ ,<sup>15</sup>  $\omega_{\text{LO}}(\text{ZnTe}) = 205 \text{ cm}^{-1}$ ,  $\omega_f(\text{ZnTe:S, local}) = 278 \text{ cm}^{-1}$ ,  $\epsilon_\infty(\text{ZnTe}) = 6.5$ ,  $\epsilon_0(\text{ZnTe}) = 9.6$ ,<sup>15</sup> and for ZnS,  $\omega_{\text{TO}}(\text{ZnS}) = 270 \text{ cm}^{-1}$ ,<sup>16</sup>  $\omega_{\text{LO}}(\text{ZnS}) = 348 \text{ cm}^{-1}$ ,  $\omega_f(\text{ZnS Te, gap}) = 200 \text{ cm}^{-1}$ ,  $\epsilon_\infty(\text{ZnS}) = 5.7$ ,  $\epsilon_0(\text{ZnS}) = 8.9$ .<sup>16</sup> The resulting force constants are  $F_{\text{Zn-Te}} = 2.42 \times 10^6$ ,  $F_{\text{Zn-S}} = 1.57 \times 10^6$ , and  $F_{\text{S-Te}} = 2.68 \times 10^6 \text{ amu/cm}^2$ . The calculated results are shown by the solid curves in Fig. 3. It can be seen that the experimental data can be well described by the MREI model and that the optical phonons of the  $\text{ZnS}_x\text{Te}_{1-x}$  mixed crystal do exhibit two-mode behavior. The ZnTe modes at  $x=1$  converge to the gap mode of Te in ZnS as  $x$  approaches 0. Similarly, the ZnS modes at  $x=0$  become the local mode of S in ZnTe as  $x$  reaches 1. At  $x=0$ , the gap mode of Te in ZnS (ZnS:Te) has

a lower frequency than the two modes of ZnS, whereas at  $x=1$ , the local mode of S in ZnTe (ZnTe:S) has a higher frequency than the two modes of ZnTe, which is expected from the fact that the mass of S is significantly smaller than that of Te.

The dependence of ZnTe-like and ZnS-like LO phonon modes on the alloy composition in  $\text{ZnS}_{1-x}\text{Te}_x$  shown in Fig. 3, could be expressed approximately by the following linear functions of  $x$ :

$$\omega(\text{ZnTe like, LO}) = 200 + 5x \text{ (cm}^{-1}\text{)},$$

$$\omega(\text{ZnS like, LO}) = 348 - 70x \text{ (cm}^{-1}\text{)}.$$

The frequency of ZnS-like LO phonons is more sensitive to the composition compared to the ZnTe-like LO phonons and is of practical use in material characterization such as the determination of alloy composition.

#### IV. CONCLUSIONS

$\text{ZnS}_{1-x}\text{Te}_x$  epilayers with different compositions were grown on (100) GaAs substrates by MBE. The x-ray diffraction spectra illustrate that the epitaxial films possess the zinc-blende structures in the whole composition range of  $0 < x < 1$ . The results of Raman studies show that the  $\text{ZnS}_{1-x}\text{Te}_x$  mixed crystals display two-mode behavior. The frequencies of long-wavelength ZnTe-like and ZnS-like optical phonons as a function of  $x$  are obtained from Raman scattering and can be well described by the MREI model.

#### ACKNOWLEDGMENT

The authors would like to thank X. L. Shen for x-ray diffraction measurements.

- <sup>1</sup>R. Hill and D. Richard, J. Phys. C **6**, L115 (1973).
- <sup>2</sup>Y. Tokumitsu, H. Kitayama, A. Kawabuchi, T. Imara, and Y. Ooka, Jpn. J. Appl. Phys. **1** **28**, 345 (1989).
- <sup>3</sup>Y. Tokumitsu, H. Kitayama, A. Kawabuchi, T. Imara, and Y. Ooka, J. Cryst. Growth **99**, 455 (1990).
- <sup>4</sup>I. K. Sou, S. M. Mou, Y. W. Chan, and G. K. L. Wong, Mater. Res. Soc. Symp. Proc. **340**, 481 (1994).
- <sup>5</sup>Y. W. Chan, H. Wang, I. K. Sou, K. S. Wong, G. K. L. Wong, J. Cryst. Growth **150**, 761 (1995).
- <sup>6</sup>I. K. Sou, K. S. Wong, Z. Y. Yang, H. Wang, and G. K. L. Wong, Appl. Phys. Lett. **66**, 1915 (1995).
- <sup>7</sup>J. W. Matthews, J. Vac. Sci. Technol. **12**, 126 (1975).
- <sup>8</sup>M. Cardona, *Light Scattering in Solid II*, edited by M. Cardona and G. Guntherodt (Springer, Heidelberg, 1982), p. 9.
- <sup>9</sup>G. Abstreiter, E. Bauser, A. Fischer, and K. Ploog, Appl. Phys. **16**, 345 (1978).
- <sup>10</sup>S. Emara, T. Nakagawa, S. Gonda, and S. Shimizu, J. Appl. Phys. **62**, 4632 (1987).
- <sup>11</sup>K. Kakimoto and T. Katoda, Appl. Phys. Lett. **40**, 826 (1982).
- <sup>12</sup>M. Ichimura, A. Usami, and T. Wada, M. Funato, K. Ichino, Sz. Fujita, and Sg. Fujita, Phys. Rev. B **46**, 4273 (1992).
- <sup>13</sup>O. Brafman, I. F. Chang, G. Lengyel, S. S. Mitra, and E. Carnall, Phys. Rev. Lett. **19**, 1120 (1967).
- <sup>14</sup>D. M. Huang, C. X. Jin, D. H. Wang, X. H. Liu, J. Wang, and X. Wang, Appl. Phys. Lett. **67**, 3611 (1995).
- <sup>15</sup>D. L. Peterson, A. Petrou, W. Giriat, A. K. Ramdas, and S. Rodriguez, Phys. Rev. B **33**, 1160 (1986).
- <sup>16</sup>I. F. Chang, and S. S. Mitra, Phys. Rev. **72**, 924 (1968).